Journal of Power Sources 235 (2013) 122–128

Contents lists available at SciVerse ScienceDirect

Journal of Power Sources

journal homepage: www.elsevier.com/locate/jpowsour

Synthesis and electrochemical performances of cobalt sulfides/graphene nanocomposite as anode material of Li-ion battery

Guochuang Huang [a], Tao Chen [b], Zhen Wang [a], Kun Chang [a], Weixiang Chen [a,*]

[a] Department of Chemistry, Zhejiang University, Hangzhou 310027, China
[b] School of Chemistry and Chemical Engineering, Yangzhou University, Yangzhou 225002, China

HIGHLIGHTS

- The cobalt sulfides/graphene composite is prepared by one-pot solvothermal route.
- The cobalt sulfides nanoparticles are highly dispersed on or wrapped in the creasy graphene.
- The composite exhibits high capacity with excellent cyclic stability and rate capability.
- We attribute the superior performances to robust composite and multiple effects of graphene.

GRAPHICAL ABSTRACT

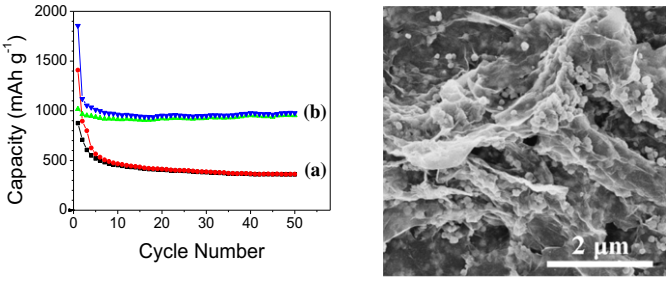

ARTICLE INFO

Article history:
Received 11 August 2012
Received in revised form
14 November 2012
Accepted 16 January 2013
Available online 13 February 2013

Keywords:
Cobalt sulfides/graphene composite
Graphene oxide sheets
Lithium ion battery
Solvothermal route

ABSTRACT

The cobalt sulfides/graphene nanosheets (GNS) composite is prepared by a facile one-pot solvothermal route in the presence of graphene oxide sheets (GOS). XRD, SEM and TEM characterizations show that sphere-like cobalt sulfides particles with an average size of about 150 nm, which are complicated phases of CoS_2, CoS and Co_9S_8, are highly dispersed on or wrapped in the creasy graphene. The selective nucleation and growth of cobalt sulfides particles on GOS make the particles more uniform in morphology and size. The as-fabricated cobalt sulfides/GNS composite exhibits very high electrochemical lithium storage reversible capacity of about 1018 mAh g^{-1}. Moreover, the cobalt sulfides/GNS composite still remains reversible capacity of above 950 mAh g^{-1} after 50 cycles at a current density of 100 mA g^{-1} as well as at the different current densities from 100 to 1000 mA g^{-1}, proving its excellent cycling durability and high-rate capability. The superior electrochemical performances of the composite may be attributed to the robust composite structure and superior conductivity, high charger mobility, large surface area and good flexibility of graphene.

1. Introductions

In recent years, considerable efforts have been devoted to the studies on the synthesis of transition metal sulfide nanomaterials due to their excellent electronic, optical and mechanical properties [1–5]. Diverse cobalt sulfide compounds with different stoichiometric compositions, such as CoS_2, CoS, Co_9S_8 and $Co_{1-x}S$, have attracted great attention due to their excellent physical, chemical, electronic and optical properties and their wide potential applications in catalysts [6,7], electrochemical supercapacitors [8–10] and Li-ion batteries [11–14]. Recently, several researchers reported the synthesis and electrochemical performances of the cobalt sulfide nanomaterials (e.g. CoS_2, CoS, Co_9S_8 and $Co_{1-x}S$) with different morphologies [6–12,15–17]. For instance, Wang et al. [15] reported the hydrothermal synthesis and structure evolution of hierarchical

* Corresponding author. Tel.: +86 571 87952477; fax: +86 571 87951895.
E-mail addresses: weixiangchen@zju.edu.cn, weixiangchen@css.zju.edu.cn (W. Chen).

0378-7753/$ – see front matter © 2013 Elsevier B.V. All rights reserved.
http://dx.doi.org/10.1016/j.jpowsour.2013.01.093

cobalt sulfide nanostructures and investigated the electrochemical behaviors of the CoS nanostructures with different morphologies as supercapacitor electrode materials. The obtained flower-like CoS exhibited a good charge/discharge performance with a high specific capacitances value of 389 F g^{-1}. Wang et al. [16] prepared the 3D flower-like CoS hierarchitectures *via* a facile one-pot solvothermal route and found that the 3D flower-like CoS hierarchitectures displayed a high discharge capacity (800–900 mAh g^{-1}) with enhanced cycle stability as Li-ion battery anode material. Furthermore, Wang et al. [17] fabricated hollow CoS_2 spheres and demonstrated that the hollow CoS_2 spheres exhibited a high specific capacity of 850 mAh g^{-1} as Li-ion battery anode materials. These valuable works demonstrate that the cobalt sulfide nanomaterials can be used as a kind of potential anode material for lithium ion battery. However, as reported by Wang et al. [16,17], the capacity of flower-like CoS decreased from 890 mAh g^{-1} to 302 mAh g^{-1} after 25 cycles and the reversible capacity of hollow CoS_2 spheres decreased from 850 mAh g^{-1} to 320 mAh g^{-1} after 40 cycles. The poor cycle stability and rate capability of the cobalt sulfides nanomaterials significantly hindered their further applications. Therefore, a new design of cobalt sulfides-based nanostructure should be developed to overcome the above defects.

As well known, two-dimensional (2D) graphene, a one-atom thick sheet of sp^2-bonded carbon, has attracted intensive interests because of their unique 2D morphology and extraordinary properties, such as superior electronic conductivity, high charge mobility, large surface area, excellent flexibility, good chemical and thermal stability, wide potential windows and others [18–20]. These properties endow graphene with multiple advantages in advanced electrochemical energy storage and conversion technology. In particular, graphene and their composites with metal oxides (e.g. SnO_2, Co_3O_4 and Fe_3O_4), Sn or Si nanoparticles have also been exploited as Li-ion battery anode materials [21–25]. The results generally show some good promises such as high specific capacity (800–1200 mA h g^{-1}) and considerable improvement in the cyclic durability of the composites [21–25]. However, very few studies have been devoted to the synthesis of cobalt sulfides/graphene composites and their electrochemical performances in Li-ion batteries. Dai et al. [7] synthesized $Co_{1-x}S$/graphene hybrid and found that the $Co_{1-x}S$/graphene hybrid displayed a high electrocatalytic activity for oxygen reduction reaction. In previous works [26–29], we have reported that hydrothermal synthesis of the transition metal dichalcogenide (MoS_2, SnS_2)/graphene composites and their excellent electrochemical properties as anode materials of Li-ion battery. Obviously, the incorporation of the graphene can enhance the electrochemical lithium storage properties and electrocatalytic activity due to the unique morphology and extraordinary physical, chemical and electronic properties. Therefore, it is expected the cobalt sulfides composites with graphene can enhance the electrochemical lithium storage properties of the composites, especially significantly improve the rate capability and cycle stability.

In this work, cobalt sulfides/graphene composite is synthesized by a facile one-pot solvothermal method and characterized by XRD, SEM and TEM. It is found that the as-prepared cobalt sulfides consisted of CoS_2, CoS and Co_9S_8 because of complex stoichiometric of cobalt chalcogenides and reactions under solvothermal conditions. Fortunately, all of these diverse cobalt sulfide compounds (CoS_2, CoS and Co_9S_8) can be used as anode materials of Li-ion batteries. The results demonstrated that the cobalt sulfides/graphene composite exhibits a very high reversible capacity (as high as 1000 mAh g^{-1}) with the excellent cycle stability and good rate capability. Even if the synthesized cobalt sulfides are complicated phases of CoS_2, CoS and Co_9S_8, the present results demonstrate that our cobalt sulfides/graphene composite exhibits the excellent electrochemical performances, and thus hold high potential as a promising anode material for high-performance Li-ion battery. The effects of graphene on the morphology of cobalt sulfides and the electrochemical performance of the cobalt sulfides/graphene composite are also investigated.

2. Experimental

2.1. Synthesis and characterizations of cobalt sulfides/graphene composite

First of all, graphene oxide was prepared by a modified Hummers' method. Natural graphite powder (Shanghai Colloid Chemical Plant, China) was poured into 50 ml of concentrated H_2SO_4 under an ice bath, then 3.00 g $KMnO_4$ was gradually added. The mixture was stirred for 2 h and then diluted with deionized water. After that, 10 ml of 30% H_2O_2 was added to the solution until the color of the mixture changed to brilliant yellow. The as-obtained graphite oxide was redispersed in deionized water and then exfoliated to generate graphene oxide sheets (GOS) by ultrasonication. A brown homogeneous supernatant was obtained by several times centrifuging and washing using deionized water and absolute ethanol.

Synthesis of cobalt sulfides/graphene composite was prepared by solvothermal route employing ethanol as solvent, cobalt dichloride ($CoCl_2 \bullet 6H_2O$) and thioaceamide (TAA) as starting materials in the presence of GOS. 0.48 g (2 mmol) of $CoCl_2 \bullet 6H_2O$ and 0.30 g (4 mmol) TAA were dissolved in ethanol under magnetic stirring. The as-made GOS was added into the solution, in which the mole ratio of $CoCl_2$ to GOS was about 1:1. The overall volume of the mixture suspension was adjusted to 80 ml by adding ethanol. After ultrasonication and stirring for 60 min, the mixture suspension was transferred into a 100 ml Teflon-lined autoclave, sealed tightly, and heated at 160 °C for 24 h. After cooling naturally, the black precipitate was collected by centrifugation, washed with deionized water and ethanol, and dried in a vacuum oven at 80 °C for 24 h. In a controlled experimental, cobalt sulfides were also prepared by above similar process without the presence of the GOS in the solution.

The morphology and structure of samples were characterized with X-ray diffraction (XRD, Thermo X'TRA X-ray diffractometer with Cu Kα-source, $\lambda = 0.15405$ nm), transmission electron microscopy (TEM; JEOL JEM-2010) and field emission scanning electron microscopy (FESEM; SIRION-100). The elemental content of the samples was analyzed by GENENIS-4000 energy dispersive X-ray spectroscopy (EDS). Raman spectra were conducted on a Jobin Yvon Labor Raman HR-800 spectrometer with argon ion laser ($\lambda = 514$ nm) in ambient air.

2.2. Electrochemical measurements

The electrochemical tests were measured using two-electrode cells assembled in an argon-filled glove box. Li sheets served as the counter electrode and reference electrode, and a polypropylene film (Celgard-2300) was used as a separator. The electrolyte was a 1.0 mol L^{-1} $LiPF_6$ solution in a mixture of ethylene carbonate/dimethyl carbonate (EC/DMC, 1:1 in volume). The working electrodes were prepared by a slurry coating procedure. The slurry consisted of 80 wt% cobalt sulfides or cobalt sulfides/graphene composite, 10 wt% acetylene black and 10 wt% polyvinylidene fluorides dissolved in *N*-methyl-2-pyrrolidinone. The obtained slurry was spread on a copper foil with diameter of 14 mm, dried at 120 °C for 12 h under a vacuum oven, and then pressed to form a working electrode. The mass of active material (cobalt sulfides or cobalt sulfides/graphene composite) was about 1.1–1.2 mg.

Galvanostatic charge/discharge cycles were carried out on a LAND CT2001 battery tester between 0.005 and 3.00 V. Electrochemical impendence spectra (EIS; PARSTAR 2273) were obtained by applying a sine wave with amplitude of 5.0 mV over the frequency range from 200 kHz to 0.01 Hz.

3. Results and discussions

3.1. Characterizations of morphology and structure

The morphology and structure of samples were investigated by XRD, SEM and TEM. Fig. 1 shows the XRD patterns of the as-synthesized cobalt sulfides and cobalt sulfides/GNS composite. As shown in Fig. 1, the diffraction peaks can be indexed to the standard diffraction data of the CoS_2 (JCPDS no. 65-3322, cubic phase), CoS (JCPDS no. 65-3418, hexagonal phase) and Co_9S_8 (JCPDS no. 65-1765, cubic phase). The fact indicates that the cobalt sulfides are complicated phases constituted of CoS_2, CoS and Co_9S_8, in stead of pure phase. Wang et al. [17] also found that the flower-like cobalt sulfides prepared by ethanol solvothermal method were a mixed phase of CoS and Co_9S_8 (9%). They suggested that it was quite difficult to obtain pure phase of cobalt sulfide because of the complex stoichiometric of cobalt chalcogenides. Yin et al. [30] found that when using $CoCl_2$ solution in mixed solution of DMSO and ethanol (volume ration of 7:3), the as-obtained cobalt sulfides consisted of CoS_2, CoS and Co_3S_4. Therefore, it is reasonable the obtained cobalt sulfides are mixed phases of CoS_2, CoS and Co_9S_8 in this work. The mixed phase cobalt sulfides consisted of CoS_2, CoS and Co_3S_4 could be converted to pure phase Co_9S_8 by annealing at 250 °C for 5 h [30]. Because the all of CoS_2, CoS and Co_9S_8 can be used as anode materials of Li-ion battery, the being annealed of the samples isn't needed in consideration of reducing process complicacy in this work. The elemental contents of the samples were determined by EDS as shown in Table 1. It can be seen that cobalt sulfides contained mostly Co and S with only a trace presence of C and O. The cobalt sulfides/GNS nanocomposite contained Co, S, C and O. The presences of C and O in the composites were clearly the contributions from reduced GO and residual oxygen-containing functional groups of reduced GO. The atomic ratio of Co:S for both samples was calculated to 1.00:(1.20–1.21), which was caused that the cobalt sulfides were the complicated phases (including CoS_2, CoS and Co_9S_8). According to the elemental contents, the weight percentage of cobalt sulfides in the composite could be estimated to be about 78.8 wt%.

Table 1
Elemental content of cobalt sulfides and cobalt sulfides/GNS composite.

Sample	Element/wt%				Composition/wt%	
	C	O	S	Co	Cobalt sulfides	GNS
Cobalt sulfides	0.89	1.78	38.71	58.62	97.33	–
Cobalt sulfides/GNS	10.00	11.18	31.10	47.72	78.82	21.18

Fig. 2 shows the SEM images of the cobalt sulfides and cobalt sulfides/GNS composite prepared by one-pot solvothermal method. As shown in Fig. 2(a) and (b), the cobalt sulfides display diverse morphologies such as sphere-like particles with broad distribution of size from 200 nm to 750 nm and thin sheets with thickness of about 120 nm. It is general that the morphology of the crystal is highly dependent on the intrinsic crystal structure. Since the cobalt sulfides prepared in this works are mixed phases of CoS_2, CoS and Co_9S_8, the cobalt sulfides display diverse morphologies. The crystal structures of CoS and Co_9S_8 are hexagonal phase, which easily results in the formation of thin sheet crystals. Wang et al. [16] reported that cobalt sulfides (mixture of CoS 91% and Co_9S_8 9%) prepared by ethanol solvothermal route displayed thin sheets and self-assembled to a flower-like morphology. As shown in Fig. 2(a), some of the cobalt sulfides sheets are also self-assembled to a flower-like morphology. Therefore, the thin sheets in Fig. 2(a) and (b) perhaps are CoS and Co_9S_8. CoS_2 is cubic phase crystal, which easily results in the formation of particles. Wang et al. [17] found that CoS_2 prepared by ethanol solvothermal route displayed nanoparticles and self-assembled to a hollow sphere. Thus, the particles with different sizes in Fig. 2(a) and (b) may be CoS_2.

As shown in Fig. 2(c) and (d), one can find that cobalt sulfides nanoparticles are uniformly wrapped in or supported on creasy graphene. In the previous work [26,27], it was found that the GOS could be easily *in-situ* reduced to creasy graphene during hydrothermal reaction using TAA as reductant. No nanosheet of cobalt sulfides can be found from Fig. 2(c) and (d). Moreover, Fig. 2(c) and (d) also shows that the all of cobalt sulfides particles in the composites exhibit uniform sphere-like morphology with an average size of 150 nm. TEM images of cobalt sulfides and cobalt sulfides/GNS composite are as shown in Fig. 3. The TEM images of cobalt sulfides/GNS composite confirm the SEM results and reveal that the sphere-like cobalt sulfides particles with an average size of 150 nm

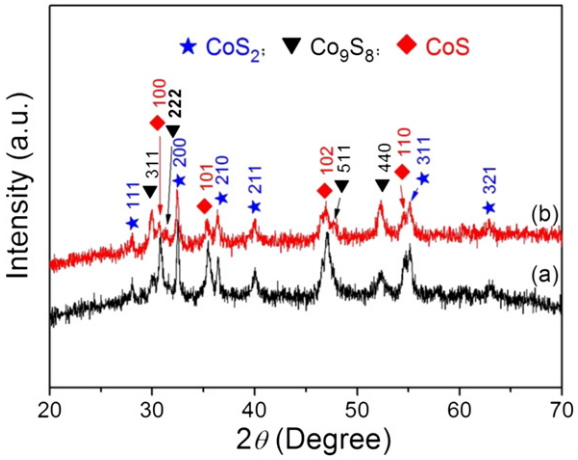

Fig. 1. XRD patterns of (a) as-synthesized cobalt sulfides and (b) cobalt sulfides/GNS composites.

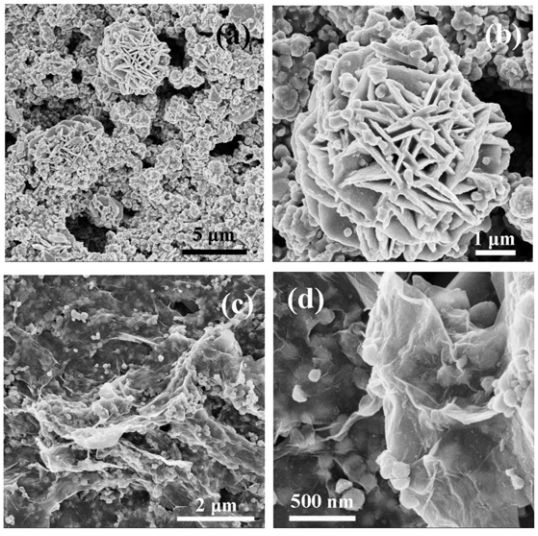

Fig. 2. SEM images of (a, b) as-synthesized cobalt sulfides and (c, d) cobalt sulfides/GNS composite.

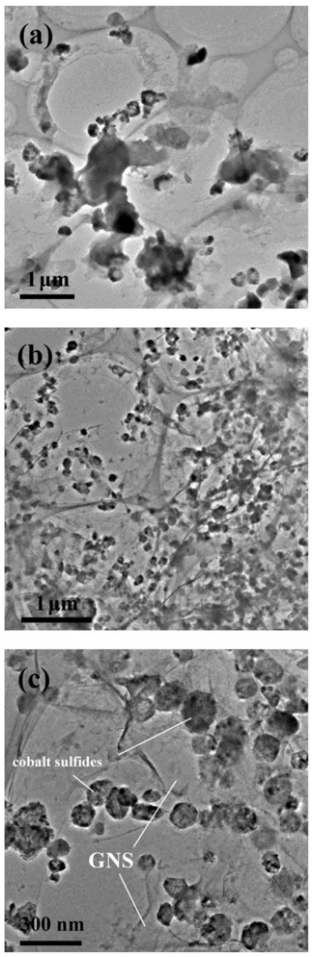

Fig. 3. TEM images of (a) cobalt sulfides and (b, c) cobalt sulfides/GNS composite.

are highly dispersed on surface and edge of graphene and the free cobalt sulfides particles are hardly found. As shown in Fig. 3(c), the graphene showing the folding nature is also clearly visible. In addition, considering that the preparation of TEM specimen is aided with the ultrasonication, the cobalt sulfides particles are still well dispersed on GNS, indicating the strong interaction between cobalt sulfides particles and GNS. In contrast, the cobalt sulfides prepared by solvothermal method in the absence of GOS or GNS exhibit very irregular morphologies and a broad size distribution as shown in Fig. 3(a). Fig. 4 shows the Raman spectroscopy of cobalt sulfides/GNS composite. There are two Raman peaks at 1355 and

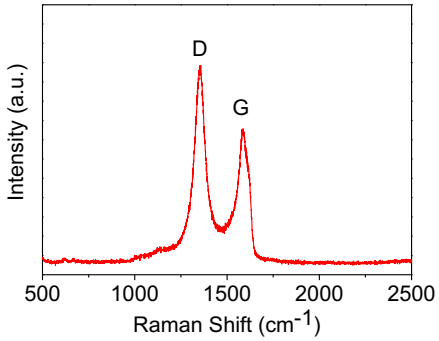

Fig. 4. Raman spectroscopy of cobalt sulfides/GNS composite.

1585 cm^{-1} for graphene, which respectively assigned to the G band (associated with the vibration of sp^2 carbon atoms in a graphitic 2D hexagonal lattice) and D band (related to the vibrations of sp^3 carbon atoms of defects and disorder) [31]. The I_D/I_G of the graphene in the composite is 1.44, which is significantly higher than that (0.93) of graphene reduced by hydrazine hydrate [32]. Decrease in the G band intensity should be attributed to the supporting of CoS_x particles on graphene surface, which may be induced by the interaction between S and C (graphene) [33–36].

It has been reported that the graphene or GOS could be used an ideal platform to growth and support other inorganic nanomaterials on their surfaces and edges [21–29]. SEM and TEM characterization (Figs. 2 and 3) reveal that the sphere-like cobalt sulfides particles with uniform morphology and size are highly dispersed on GNS surfaces and edges. We investigate the mechanism for the formation of cobalt sulfides/GNS composite as schematized in Fig. 5. It is well known that Co^{2+} ion can easily coordinate with −COOH, −OH and −C═O. Because there are a lot of oxygen-containing functional groups on the surfaces and edges of GOS, Co^{2+} ion can be very easily absorbed on the GOS by the coordinate interaction between the oxygen-containing functional groups on GOS and Co^{2+} ion. Therefore, the nucleation and subsequent growth of cobalt sulfides are selective on GOS surfaces and edges, with little free particle growth in solution. The selective nucleation and growth of cobalt sulfides on GOS restrain their overgrowth and aggregation. Thus, cobalt sulfides particles in/on graphene display a uniform sphere-like morphology with a narrow size distribution. Wang et al. [16] has reported that the CoS nanosheets was produced by aggregation of CoS nanoparticles formed in early stage (4.0–8.0 h) of solvothermal reaction. Since the aggregation of cobalt sulfides particles is restrained because of selective nucleation and growth of cobalt sulfides crystals on GOS, sphere-like cobalt sulfides particles cannot aggregate to thin sheets. Thus, there is no cobalt sulfide thin sheets in the cobalt sulfides/GNS composite as shown in Fig. 2(c) and (d) and Fig. 3(b) and (c).

3.2. Electrochemical performances

Fig. 6 shows the first three charge and discharge curves of cobalt sulfides and cobalt sulfides/GNS composite electrodes at a constant current density of 100 mA g^{-1} (0.1 C-rate). As shown in Fig. 6a, the first discharge curve (lithiation) of cobalt sulfides electrode displays a short flat voltage at 1.62 V and an obvious flat voltage at 1.35 V, respectively, which represent the insertion of a small amount of lithium ion to form lithiated cobalt sulfides and the decomposition of lithiated cobalt sulfides or cobalt sulfides into Co metal and Li_2S [17]. The slope from 1.0 V to 5 mV might be attributed to the formation of a surface polymer layer [16] and/or lithium storage within the interfaces between two distinct phase of Co and Li_2S [37], which in general contribute to addition capacity. The charge curves (delithiation) of cobalt sulfides display two plateau potentials at about 1.95 V and 2.32 V, respectively, in good agreement with the work reported by Wang et al. [17]. The two plateau potentials at 1.95 V and 2.32 V respectively correspond to the partial oxidation of Co to form metal sulfides and delithiation of Li_2S ($Li_2S - 2e^- = 2Li^+ + S$) [37]. In the first cycle, cobalt sulfides deliver a discharge capacity of 1408 mAh g^{-1} and reversible capacity of 875 mAh g^{-1}, which well agree with that of flower-like CoS (890 mAh g^{-1}) [16] and CoS_2 hollow spheres (900 mAh g^{-1}) [17]. The irreversible capacity in the first cycle may be attributed to the formation of solid-electrolyte interface (SEI) film on the surface of the electrode materials and other irreversible decomposition reaction. As shown in Fig. 6b, the first discharge curve of cobalt sulfides/GNS composite electrode also displays a short flat voltage at 1.65 V, two obvious flat voltages at 1.35 V and 0.75 V. The flat

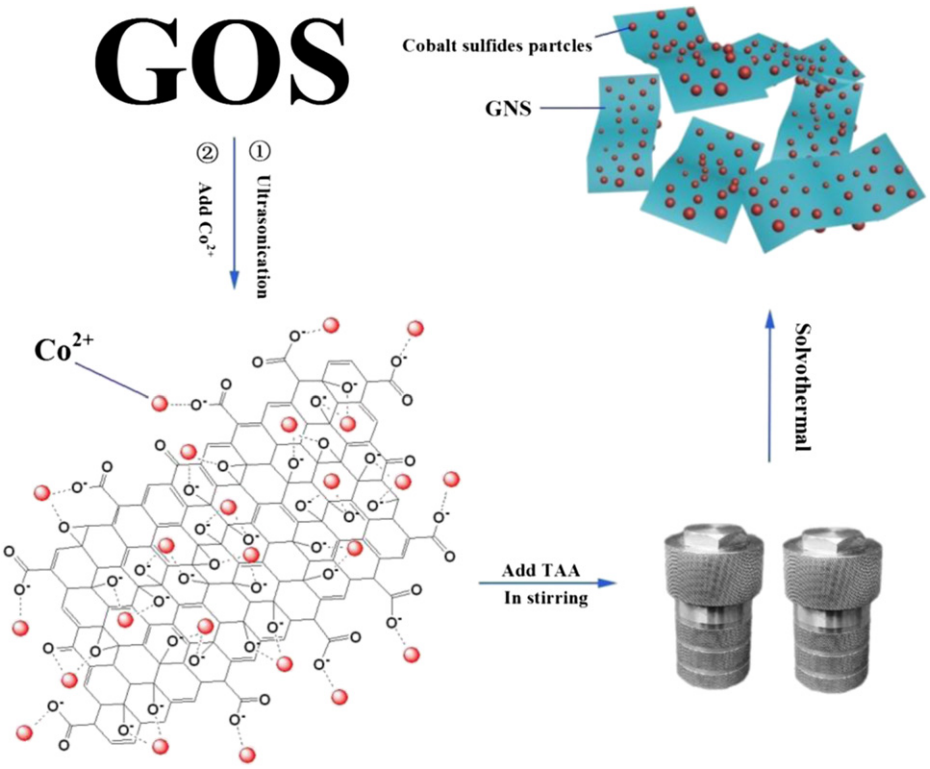

Fig. 5. Schematic of the synthesis route of the cobalt sulfides/GNS composite by one-pot solvothermal method.

voltages at 1.65 V and 1.35 V represent respectively the insertion of a small amount of lithium ion into cobalt sulfides and the decomposition reaction into Co and Li_2S [17,37]. As well known, the plateau potential at about 0.8 V at the first discharge process for carbon materials is generally attributed to the formation of SEI film. Therefore, this flat voltage at 0.75 V should be related to the formation of SEI film on GNS surface. The shorter flat voltages at 0.75 V in the 2nd and 3rd discharge curves than that at the 1st discharge curve can be still observed, which correspond to electrochemically lithium storage of graphene [38]. The charge curves of cobalt sulfides/GNS composite display there plateau potentials at about 1.2 V, 1.9 V and 2.3 V. The two plateau potentials at about 1.95 V and 2.30 V correspond to delithiation process of cobalt sulfides in the composite, which agree on the whole with cobalt sulfides electrode. Thus the plateau potentials at 1.2 V should correspond to electrochemical delithiation of graphene. In the first cycle, the cobalt sulfides/graphene composite delivers a discharge capacity of 1855 mAh g^{-1} and reversible capacity of 1018 mAh g^{-1}. The irreversible capacity in the first cycle also is attributed to the formation of SEI film and other irreversible decomposition reaction. In a word, the cobalt sulfides/GNS composite exhibits a high reversible specific capacity of 1018 mAh g^{-1}, which is larger than that of cobalt sulfides prepared in this work, and also larger than that of flower-like CoS (890 mAh g^{-1}) [16] and CoS_2 hollow spheres (900 mAh g^{-1}) [17]. Our previous work has reported [29] that the GNS delivered a reversible specific capacity of 887 mAh g^{-1} at the first cycle. According to the weight compositions of cobalt sulfides in the cobalt sulfides/GNS composite, we could calculate that the specific capacity of cobalt sulfides is 1053 mAh g^{-1}, which was much higher than their theoretical capacity (CoS_2: 870 mAh g^{-1}; CoS: 590 mAh g^{-1} and Co_9S_8: 540 mAh g^{-1}). Therefore, such a high specific capacity of the composite could be attributed to the multiple positive effects of graphene and the synergism between graphene and cobalt sulfides.

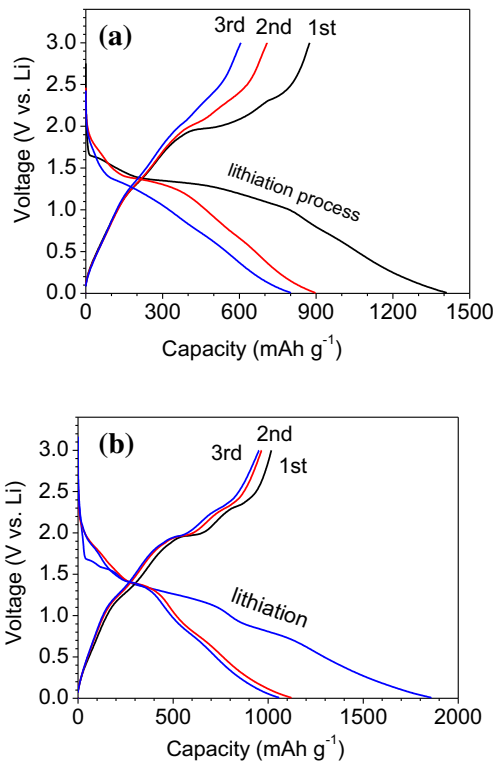

Fig. 6. First three charge and discharge curves of (a) cobalt sulfides and (b) cobalt sulfides/GNS composite electrodes.

Fig. 7 illustrates the charge/discharge capacity of cobalt sulfides and cobalt sulfides/GNS composite electrodes as function of the cycle number. As shown in Fig. 7, the first discharge capacities (lithiation) of the cobalt sulfides and cobalt sulfides/GNS composite are 1408 and 1855 mAh g^{-1}, respectively, while the first delithiation

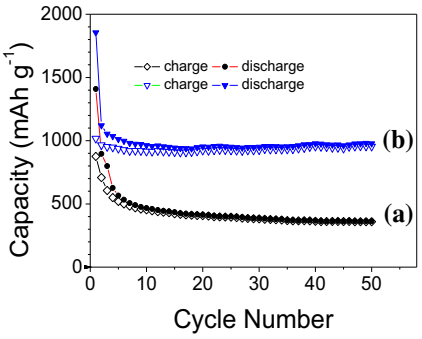

Fig. 7. Cycling behavior of (a) cobalt sulfides and (b) cobalt sulfides/GNS composite electrodes at a current density of 100 mA g^{-1}.

(charge) capacities are 885 and 1018 mAh g^{-1}, respectively. It was demonstrated that the graphene composites with metal oxides or metal sulfides such as SnO_2/GNS [21], MoS_2/GNS [28] and SnS_2/GNS [29,39] delivered a very high reversible specific capacity as anode materials of Li-ion battery due to multiple positive effects of graphene and robust composite structure. In this work, the cobalt sulfides/GNS composite exhibits reversible capacity as high as 1018 mAh g^{-1}. More importantly, Fig. 7 reveals that the cobalt sulfides/GNS composite electrode displays an excellent cyclic stability in comparison with cobalt sulfides. In addition, the cyclic stability of cobalt sulfides/GNS composite in this work is also much better than that of flower-like CoS and hollow CoS_2 reported by Wang et al. [16,17]. As shown in Fig. 7, the reversible capacity of the composite hardly decreases with increasing cycles and the reversible capacity of 954 mAh g^{-1} is remained after 50 cycles. Although for the cobalt sulfides electrode, the initial reversible capacity of 875 mAh g^{-1} is not low, but the capacity of only 359 mAh g^{-1} is remained after 50 cycles.

The high reversible capacity and excellent cycling behavior of the cobalt sulfides/GNS composite are also exhibited in the rate capability. Fig. 8 shows the capacity of the cobalt sulfides and cobalt sulfides/GNS composites at different rates (1 C-rate = 1000 mA g^{-1}). As shown in Fig. 8, the cobalt sulfides/GNS composite electrode demonstrates much better rate capability than cobalt sulfides electrode. Even at a high current density of 1000 mA g^{-1}, the cobalt sulfides/GNS composite electrode remains with the specific capacity of 680 mAh g^{-1}, which is much higher than that of cobalt sulfides. Additionally, the cobalt sulfides/GNS composite exhibits the good cycling stability at different charge/discharge current densities. As shown in Fig. 8b, when the current density changes from 1000 to 100 mA g^{-1}, the specific capacity of the sulfides/GNS composite returns to the last value at low current density of 100 mA g^{-1} and

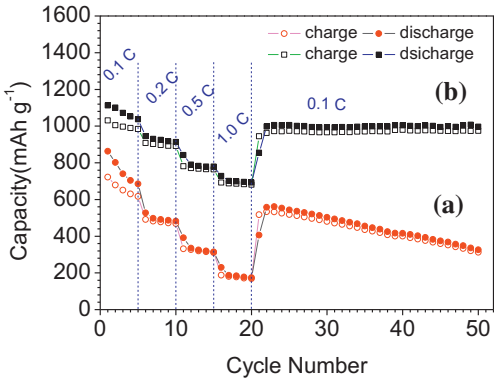

Fig. 8. Rate capability of (a) cobalt sulfides and (b) cobalt sulfides/GNS composite electrode at different rates (1 C-rate = 1000 mA g^{-1}).

does not ultimately change in the subsequent cycles, indicating its excellent cycling stability. As shown in Fig. 8, after 50 cycles at different charge–discharge current densities, the cobalt sulfides/GNS composite electrode remains reversible capacity of 973 mAh g^{-1}, while the cobalt sulfides electrode remains reversible capacity of only 312 mAh g^{-1}. It is evidently demonstrated that the cobalt sulfides/GNS composite exhibits higher reversible capacity, better rate capability and excellent cyclic stability in comparison with cobalt sulfides.

We attribute the superior electrochemical performances of the cobalt sulfides/GNS composite to extraordinary properties of graphene and the robust composite structure. It was demonstrated that the electron transfer rate of graphene electrode was more than 10-fold faster than basal plane of bulk graphite due to the presence of corrugations on the graphene sheets [40]. The high electronic conductivity and charge mobility of graphene would not only greatly reduce contact resistance of composite electrode, but also significantly enhanced rapid transfer of electron during electrode reaction. As shown in Figs. 2 and 3, the creasy graphene sheets with high surface specific area could provide an ideal matrix for highly dispersion of small cobalt sulfides particles, more available space for electrolyte access and more short-path for lithium ion diffusion. Thus the cobalt sulfides/GNS composite electrode exhibits high reversible lithium storage capacity and good high-rate capability. In addition, the good flexibility of graphene can effectively buffer the volume change of electrochemical active material and stabilize composite structure of electrode during long charge/discharge cycles, resulting in the excellent cyclic durability.

In order to gain better understanding of why cobalt sulfides/GNS composite exhibits such a superior electrochemical performance compared to cobalt sulfides electrode, EIS measurements were performed as shown in Fig. 9a. An equivalent circuit is also shown in Fig. 9b in accordance with the reported works [41]. R_e represents the internal resistance of the test battery, R_f and CPE_1 are related to the contact resistance and constant phase element of SEI film, R_{ct} and CPE_2 are related to the charge-transfer resistance and constant phase element of the electrode/electrolyte interface, Z_W is related to the Warburg impedance corresponding to the lithium ion diffusion process. As shown in Fig. 9a, the high frequency semicircle is

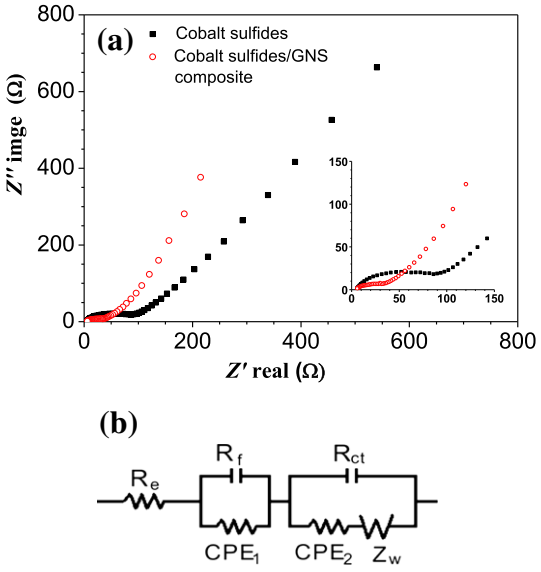

Fig. 9. (a) Nyquist plots of cobalt sulfides and cobalt sulfides/GNS composite electrodes obtained by applying a sine wave with amplitude of 5.0 mV over the frequency range from 100 kHz to 0.01 Hz; (b) equivalent circuit model of the studied system, CPE represent the constant phase element, $Z_{CPE} = \{Q(j\omega)^n\}^{-1}$, $0 < n < 1$.

Table 2
Impedance parameters derived using equivalent circuit model for cobalt sulfides and cobalt sulfides/GNS composite electrodes.

Electrode	R_e/Ω	R_f/Ω	Q_1/μF	n_1	R_{ct}/Ω	Q_2/μF	n_2
Cobalt sulfides	4.86	26.5	24.2	0.738	58.5	217.3	0.603
Cobalt sulfides/GNS	4.71	5.48	49.6	0.730	27.1	996.4	0.475

corresponding to the contact resistance R_f and CPE_1 of SEI film, the semicircle in medium frequency region is allocating the charge-transfer resistance R_{ct} and CPE_2 of electrode/electrolyte interface, and the inclined line approached to about 45–50° angle to the real axis is corresponding to the lithium-diffusion process. The kinetic differences of cobalt sulfides and cobalt sulfides/GNS composite electrodes were further investigated by fitting of EIS based on the equivalent circuit model in Fig. 9b. The fitted impedance parameters of two electrodes are listed in Table 2. It shows that the R_f and R_{ct} of cobalt sulfides/GNS electrode are 5.48 Ω and 27.1 Ω, respectively, which are significantly lower than those of cobalt sulfides electrode (R_f = 26.5 Ω and R_{ct} = 58.5 Ω). The result confirms that that GNS can not only greatly reduce the contact resistance of composite electrode, but also significantly enhances rapid electron transfer, resulting in the significant improvement in the kinetic performance of electrochemical lithium insertion/extraction. Therefore, the cobalt sulfides/GNS composite electrode exhibits considerably enhanced capacity with excellent cyclic stability and high-rate capability.

4. Conclusions

This work describes a facile one-pot solvothermal method for synthesis of the cobalt sulfides/GNS composite, in which graphene oxide sheets provide an ideal platform for the selective nucleation and growth of cobalt sulfides particles. It is demonstrated that the sphere-like cobalt sulfides particles with uniform size are highly dispersed on or wrapped in the creasy graphene. The graphene has an evidently influence on the morphology of cobalt sulfides and makes the particles more uniform in morphology and size because of the selective nucleation and growth of cobalt sulfides on GOS. Even although the cobalt sulfides in composite are complicated phases of CoS_2, CoS and Co_9S_8, the cobalt sulfides/GNS composite displays much higher reversible capacity of about 1010 mAh g^{-1} with better rate capability and excellent cyclic stability than the cobalt sulfides. We attribute the significant improvement in electrochemical performances of the composite to the multiple positive effects of graphene and the robust composite structure. EIS analysis confirms that the incorporation of graphene preserves the high conductivity and greatly enhances the electron rapid transfer of the cobalt sulfides/GNS composite electrode during electrochemical reaction. The present results suggest that the cobalt sulfides/GNS composite can be used as a promising anode material for high-performance Li-ion battery.

Acknowledgments

This work is financially supported by the Natural Science Foundation of China (21173190), the International Science and Technology Cooperation Program of China (2012DFG42100), the Doctoral Program of Higher Education of China (2011010113003), the Zhejiang Provincial Natural Science Foundation of China (Y4100119) and the Science and Technology Department of Zhejiang Province (2011C21024).

References

[1] R. Tenne, Angew. Chem. Int. Ed. 42 (2003) 5124–5132.
[2] P.G. Li, M. Lei, X.F. Wang, H.L. Tang, W.H. Tang, J. Alloys Compd. 474 (2008) 463–467.
[3] J. Heising, M.G. Kanatzidis, J. Am. Chem. Soc. 121 (1999) 11720–11732.
[4] A. Rothschild, J. Sloan, R. Tenne, J. Am. Chem. Soc. 122 (2000) 5169–5179.
[5] D.W. Song, Q.H. Wang, Y.P. Wang, Y.J. Wang, Y. Han, L. Li, G. Liu, L.F. Jiao, H.T. Yuan, J. Power Sources 195 (2010) 7462–7465.
[6] R.C. Hoodless, R.B. Moyes, P.B. Wells, Catal. Today 114 (2006) 377–382.
[7] H.L. Wang, Y.Y. Liang, Y.G. Li, H.J. Dai, Angew. Chem. Int. Ed. 50 (2011) 10969–10972.
[8] P. Justin, G.R. Rao, Int. J. Hydrogen Energy 35 (2010) 9709–9715.
[9] Q.H. Wang, L.F. Jiao, H.M. Du, J.Q. Yang, Q.N. Huan, W.X. Peng, Y.C. Si, Y.J. Wang, H.T. Yuan, CrystEngComm 13 (2011) 6960–6963.
[10] W.J. Dong, X.B. Wang, B.J. Li, L.N. Wang, B.Y. Chen, C.R. Li, X.A. Li, T.R. Zhang, Z. Shi, Dalton Trans. 40 (2011) 243–248.
[11] R.D. Apostolova, E.M. Shembel, I. Talyosef, J. Grinblat, B. Markovsky, D. Aurbach, Russ. J. Electrochem. 45 (2009) 311–319.
[12] Y. Kim, J.B. Goodenough, J. Phys. Chem. C 112 (2008) 15060–15064.
[13] A. Debart, L. Dupont, R. Patrice, J.M. Tarascon, Solid State Sci. 8 (2006) 640–651.
[14] P.J. Masset, R.A. Guidotti, J. Power Sources 178 (2008) 456–466.
[15] J. Wang, S.H. Ng, G.X. Wang, J. Chen, L. Zhao, Y. Chen, H.K. Liu, J. Power Sources 159 (2006) 287–290.
[16] Q.H. Wang, L.F. Jiao, H.M. Du, W.X. Peng, Y. Han, D.W. Song, Y.C. Si, Y.J. Wang, H.T. Yuan, J. Mater. Chem. 21 (2011) 327–329.
[17] Q.H. Wang, L.F. Jiao, Y. Han, H.M. Du, W.X. Peng, Q.N. Huan, D.W. Song, Y.C. Si, Y.J. Wang, H.T. Yuan, J. Phys. Chem. 115 (2011) 8300–8304.
[18] C. Lee, X.D. Wei, J.W. Kysar, J. Hone, Science 321 (2008) 385–388.
[19] Y.M. Lin, C. Dimitrakopoulos, K.A. Jenkins, D.B. Farmer, H.Y. Chiu, A. Grill, P. Avouris, Science 327 (2010) 662.
[20] A.S. Arico, P. Bruce, B. Scrosati, J.M. Tarascon, Nat. Mater. 4 (2005) 366–377.
[21] H.D. Liu, J. Huang, X.L. Li, J. Liu, Y.X. Zhang, K. Du, Appl. Surf. Sci. 258 (2012) 4917–4921.
[22] L.Q. Tao, J.T. Zai, K.X. Wang, H.J. Zhang, M. Xu, J. Shen, Y.Z. Su, X.F. Qian, J. Power Sources 202 (2012) 230–235.
[23] Y.J. Mai, S.J. Shi, D. Zhang, Y. Lu, C.D. Gu, J.P. Tu, J. Power Sources 204 (2012) 155–161.
[24] S.K. Behera, Chem. Commun. 47 (2011) 10371–10373.
[25] S.N. Yang, G.R. Li, Q. Zhu, Q.M. Pan, J. Mater. Chem. 22 (2012) 3420–3425.
[26] K. Chang, W.X. Chen, Chem. Commun. 47 (2011) 4252–4254.
[27] K. Chang, W.X. Chen, J. Mater. Chem. 21 (2011) 17175–17184.
[28] K. Chang, W.X. Chen, ACS Nano 5 (2011) 4720–4728.
[29] K. Chang, Z. Wang, G.C. Huang, H. Li, W.X. Chen, J.Y. Lee, J. Power Sources 201 (2012) 259–266.
[30] P.F. Yin, L.L. Sun, Y.L. Gao, S.Y. Wang, Bull. Mater. Sci. 31 (2008) 593–596.
[31] M. Dehonor, K. Varlot-Masenelli, A. Gonzalez-Montiel, C. Gauthier, J.Y. Cavaille, H. Terrones, M. Terrones, Chem. Commun. (2005) 5349–5351.
[32] O.A. Vargas C, A. Caballero, J. Morales, Nanoscale 4 (2012) 2083–2092.
[33] M.S. Dresselhaus, A. Jorio, M. Hofmann, G. Dresselhaus, R. Saito, Nano Lett. 10 (2010) 751–758.
[34] S. Dannefaer, A. Pu, V. Avalos, D. Kerr, Phys. B Condens. Matter 308–310 (2001) 569–572.
[35] H.X. Xu, X.B. Wang, Y.F. Zhang, S.Y. Liu, Chem. Mater. 18 (2006) 2929–2934.
[36] Y. Lin, B. Zhou, K.A.S. Fernando, P. Liu, L.F. Allard, Y.P. Sun, Macromolecules 36 (2003) 7199–7204.
[37] X.P. Fang, X.Q. Xu, S.F. Liao, Y.F. Shi, Y.S. Hu, Z.X. Wang, G.D. Stucky, L.Q. Chen, Microporous Mesoporous Mater. 151 (2012) 418–423.
[38] P. Guo, H.H. Song, X.H. Chen, Electrochem. Commun. 11 (2009) 1320–1324.
[39] M. Sathish, S. Mitani, T. Tomai, I. Honma, J. Phys. Chem. 116 (2012) 12475–12481.
[40] W. Li, C. Tan, M.A. Lowe, H.D. Abruna, D.C. Ralph, ACS Nano 5 (2011) 2264–2270.
[41] S.B. Yang, H.H. Song, X.H. Chen, Electrochem. Commun. 8 (2006) 137–142.